Direct and High-Throughput Assays for Human Cell Killing through Trogocytosis by Entamoeba histolytica

Akhila Bettadapur[1], **Katherine S. Ralston**[1,*]

[1]Department of Microbiology and Molecular Genetics, University of California, Davis, USA

Abstract

Entamoeba histolytica is the causative agent of amoebiasis. Pathogenesis is associated with profound damage to human tissues. We previously showed that amoebae kill human cells through trogocytosis. Trogocytosis is likely to underlie tissue damage during infection, although the mechanism is still unknown. Trogocytosis is difficult to assay quantitatively, which makes it difficult to study. Here, we developed two new, complementary assays to measure trogocytosis by quantifying human cell death. One assay uses CellTiterGlo, a luminescent readout for ATP, as a proxy for cell death. We found that the CellTiterGlo could be used to detect death of human cells after co-incubation with amoebae, and that it was sensitive to inhibition of actin or the amoeba surface Gal/GalNAc lectin, two conditions that are known to inhibit amoebic trogocytosis. The other assay uses two fluorescent nuclear stains to directly differentiate live and dead human cells by microscopy, and is also sensitive to inhibition of amoebic trogocytosis through interference with actin. Both assays are simple and inexpensive, can be used with suspension and adherent human cell types, and are amenable to high-throughput approaches. These new assays are tools to improve understanding of trogocytosis and amoebiasis pathogenesis.

Graphical Abstract

Entamoeba histolytica kills human cells by performing trogocytosis. We developed new trogocytosis assays. One assay uses fluorescent nuclear stains to differentiate live (blue) and dead (turquoise) human cells.

Entamoeba histolytica is the causative agent of amoebiasis and is responsible for approximately 50 million infections/year [1]. 80% of infants in an urban slum in Dhaka, Bangladesh are infected with *E. histolytica* [2]. Amoebiasis results in 15,500 deaths/year in children and 67,900 deaths/year among people of all ages [3]. During infection, the actively replicating trophozoite (amoeba) form colonizes the large intestine. Symptoms range from asymptomatic infection, diarrhea, bloody diarrhea, to fatal extraintestinal abscesses. The species name (*histo-*: tissue; *lytic-*: dissolve) refers to the capacity of the amoeba to damage human tissues. However, it is still unclear how amoebae invade and damage tissues. The contact-dependent human-cell killing activity of *E. histolytica* [4, 5] is likely to be a major contributor to human tissue damage.

While it has been under investigation for many years, the mechanism by which amoebae kill human cells was previously unclear [6]. We defined that amoebae kill human cells *via* trogocytosis (*trogo-:* nibble) [7]. Amoebae attached to human cells and then physically extract "bites" of human cell membrane, cytoplasm and organelles, which eventually lead to human cell death. Amoebic trogocytosis required engagement of the Gal/GalNAc lectin, actin rearrangements, PI3K and EhC2PK signaling [7]. Amoebic trogocytosis was necessary for invasion of *ex vivo* intestinal tissue, underlining its relevance to pathogenesis [7].

Trogocytosis might be evolutionarily-conserved [8], therefore, studying this process in *E. histolytica* may give insight into eukaryotic trogocytosis, in addition to a better understanding of the pathogenesis of amoebiasis.

In order to better understand trogocytosis and its contribution to disease, robust cell death assays are needed. Trogocytosis is difficult to assay directly, since direct visualization of this process using microscopy is necessary. The major challenge of microscopy-based approaches is that it is necessary to apply unbiased quantification to ensure that the results are robust and reproducible. We previously used imaging flow cytometry to measure trogocytosis quantitatively [7]. In this assay, amoebae and human cells are fluorescently labeled, allowing trogocytosis to be directly measured, and Live/Dead Violet is used to stain dead (permeable) cells [7, 9, 10]. This assay allows for automated analysis of thousands of images per sample, but is limited in practicality since imaging flow cytometers are not widely available. This assay is more easily applied to study suspension cells, since cells must be in suspension during image acquisition; thus, imaging flow cytometry is limited in flexibility. While samples can be acquired from 96-well plates, imaging flow cytometry is not a truly high-throughput approach.

Cell death assays that can be applied to high-throughput techniques, like screening for small molecule inhibitors of trogocytosis, would be a useful addition to the assays in current use. Assaying human cell killing by *E. histolytica* is inherently challenging since readouts must specifically measure the viability of the human cells when they are mixed together with amoebae. While amoebae can kill essentially any human cell type [11], most studies have focused on either monolayers or suspension cultures, but not both, since they are typically not amenable to the same assays. Thus, flexible assays that can be applied to both monolayers and suspension cells would be beneficial.

Assays that have been previously used can be broken down into membrane permeabilization, monolayer disruption, and apoptosis assays. Membrane permeabilization assays detect intracellular components that are released into the culture supernatant by dead cells. In these assays, amoebae are co-incubated with human cells, and the supernatant is measured. LDH assays [12, 13] generally use NAD to catalyze a reporter reaction [14]. This means that other enzymatic activities in the supernatant that use NAD as a cofactor can be problematic. By contrast, the ^{51}Cr release assay specifically measures host cell death, since in this assay, host cells are pre-labeled with ^{51}Cr, and after incubation with amoebae, ^{51}Cr in the culture supernatant is measured [15, 16].

Monolayer disruption assays are commonly used [17]. In these assays, amoebae are incubated with monolayers, and after washing, the remaining cells are detected by methylene blue staining [18, 19]. Similarly, calcein AM has been pre-loaded into monolayers and, after co-incubation with amoebae and washing, calcein AM signal is used as a readout for the remaining cells [20]. Trypan blue staining has also been used to stain dead cells remaining in monolayers [21, 22]. However, since amoebic proteases cause disruption of monolayers [17] and these assays call for wash steps after co-incubation with amoebae, protease activity can confound interpretation.

Finally, apoptosis assays have been used to study cell killing by amoebae [16, 23]. In some assays, care is needed to ensure the readout is specific to apoptosis. For example, DNA laddering can occur in other modes of cell death besides canonical apoptosis [24]. Annexin V staining to detect exposed phosphatidylserine should be combined with cell permeability stains like propidium iodide, to ensure that phosphatidylserine exposure is not the result of membrane damage. Apoptosis assays capture markers of apoptosis in dying cells, which differs from other cell death assays that measure cell death after it has occurred.

Here we developed two new, complementary assays for human cell death. We showed that CellTiterGlo, a luminescent readout for cellular ATP levels, can be used as a proxy for human cell viability. We also developed a confocal microscopy-based assay with fluorescent nuclear stains that quantitatively differentiate live and dead human cells. Both assays were sensitive to conditions that are known to inhibit amoebic trogocytosis. Both assays are simple and inexpensive, can be used with suspension and adherent human cell types, and can be applied to high-throughput studies.

CellTiterGlo is a very simple, high-throughput luminescent assay for cell viability that is based on cellular ATP levels. Assays for human cell killing by amoebae typically use an amoeba to human cell ratio between 1:10 and 1:40. We reasoned that since the number of human cells exceeds the number of amoebae, human cells should contribute to the majority of the CellTiterGlo luminescence signal. We first asked whether luminescence values correlated with the number of amoebae (Fig. 1A) or human Jurkat T cells per well (Fig. 1B), and found that luminescence was correlated with cell number.

Next, amoebae and Jurkat cells were co-incubated, or incubated alone as controls. In control samples, equivalent numbers of cells were loaded per well to correspond to the number of cells present in the co-incubation. As anticipated, the luminescence values were higher for control human cells than for amoebae (Fig. 1C – 1D). The luminescence values of human cells typically decreased slightly at the start of the assay, and recovered over time. When human cells and amoebae were co-incubated, the luminescence value initially corresponded to roughly the sum of the human cell and amoeba individual values, and then decreased over time. The luminescence values of the co-incubation were significantly lower than the values for human cells incubated alone (Fig. 1D). Reduced variability was observed when samples were incubated in an anaerobic GasPak (Fig. 1C – 1D), compared to an aerobic environment (Fig. S1), consistent with the microaerophilic metabolism of *E. histolytica.*

We next asked whether this assay was sensitive to conditions that inhibit amoebic trogocytosis. We have previously shown that amoebae kill Jurkat cells by performing trogocytosis, and that trogocytosis is inhibited by treatment with Cytochalasin D [7]. Therefore, Cytochalasin D-treated or DMSO control-treated amoebae were co-incubated with Jurkat cells, and cell viability was measured using CellTiterGlo (Fig. 1E – F). Cytochalasin D-treated amoebae were significantly less able to kill human cells, as seen by the increased CellTiterGlo signal compared to control amoebae (Fig. 1E – F). For human cells or amoebae incubated alone, Cytochalasin D treatment did not affect viability (Fig. S2A).

Amoeba must attach to human cells in order to kill them, and this attachment is mediated by the amoebic GalNAc lectin [25]. We have previously shown that engagement of the amoeba surface Gal/GalNAc lectin is necessary for trogocytosis [7]. We next tested if CellTiterGlo was sensitive to inhibition of the Gal/GalNAc lectin. Galactose-treated amoebae were significantly less able to kill human cells, compared to control mannose-treated amoebae (Fig. 1G, S2B – C). Finally, we tested knockdown mutant amoebae deficient in a rhomboid protease, EhRom1, which has a characterized role in attachment to human cells [26, 27]. There was no significant difference in the cell killing ability between EhRom1 knockdown mutants and vector control amoebae (Fig. 1H, S2D – E). This is consistent with the lack of a trogocytosis defect in EhRom1 mutants [10]. Taken together, we concluded that the CellTiterGlo assay is sensitive to the inhibition of amoebic trogocytosis.

We next sought to extend this assay to other human cell types, since many assays for cell killing are difficult to adapt to both suspension and monolayer cells. Therefore, we adapted the CellTiterGlo assay to human Caco-2 intestinal epithelial cell monolayers. CellTiterGlo luminescence values correlated closely with the number of amoebae or Caco-2 cells per well (Fig. 2A – 2B). Due to washing steps and the addition of fresh media, the luminescence values of Caco-2 cells typically decreased slightly at the start of the assay, and recovered over time. When Caco-2 cells and amoebae were co-incubated, the luminescence value initially corresponded to roughly the sum of the human cell and amoeba individual values (Fig. 2C). The luminescence values of the co-incubation were significantly lower than the values for human cells incubated alone (Fig. 2D). These results show that CellTiterGlo can be applied to assay killing of both suspension and monolayer cells.

We next developed a microscopy-based assay to directly measure human cell killing by amoebae. Since human cell nuclei are not internalized during amoebic trogocytosis [7], we devised a strategy with two different nuclear stains to distinguish living and dead human cells. Human cell nuclei were pre-labeled with Hoechst prior to co-incubation. Amoebae were not labeled with Hoechst or other dyes. During co-incubation, SYTOX green was present in the media. SYTOX green is a nucleic acid stain that is excluded by living cells, but is taken up by dead cells because they have permeable membranes. Thus, live human cells are labeled only by Hoechst, while dead human cells are dual-labeled by both Hoechst and SYTOX green (Video S1). To test this dual-stain assay, Cytochalasin D treatment was used to inhibit amoebic trogocytosis. Amoebae were treated with Cytochalasin D or DMSO, and co-incubated with human Jurkat T cells (Fig. 3A). Cytochalasin D-treated amoebae killed less than 2% of Jurkat cells in 60 minutes (Fig. 3B). By comparison, control amoebae killed 40% of Jurkat cells in 60 minutes. This assay provides a quantitative readout for cell killing, and it is robust enough to be amenable to imaging large fields of cells at low magnification (Fig. 3C). Finally, this dual-stain assay can be applied to Caco-2 epithelial cells (Fig. 3D, S3, and Videos S2 – S3), demonstrating that it is versatile with respect to human cell types.

In this study, we developed two assays for human cell killing by *E. histolytica.* The CellTiterGlo assay biochemically measures cellular ATP levels, and the dual-stain microscopy assay allows for direct visualization of human cell death with fluorescent stains.

These assays complement the currently available cell death assays and bring their own unique strengths and weaknesses.

Trogocytosis is difficult to assay directly. In order to detect and differentiate trogocytosis from other processes, microscopy is necessary. We used microscopy to initially characterize *E. histolytica* trogocytosis [7]. The challenge is that it is necessary to apply unbiased quantification to ensure that microscopy results are robust and reproducible. We previously used imaging flow cytometry to directly detect and quantify trogocytosis [7]. For microscopy approaches, imaging flow cytometry is the most high-throughput and robust way to quantify images. However, this approach is limited in practicality since imaging flow cytometers are not widely available. The new assays that we developed do not take the place of image-based detection of trogocytosis, but they complement these approaches, by providing a high-throughput option and a practical solution for researchers that do not have access to imaging flow cytometry or high-resolution microscopes for direct imaging of trogocytosis.

The CellTiterGlo assay is simple and practical. Only a plate reader is required for the readout. The assay requires few manipulations and no washing steps after co-incubation; CellTiterGlo solution is added directly to cells, and after a brief incubation, luminescence is measured on a plate reader. Since there are no washing steps after co-incubation, this assay helps to overcome the challenges related to amoebic protease activity, that have confounded interpretation of monolayer disruption assays in previous studies. In the CellTiterGlo assay, even if protease activity causes human cells to be released from monolayers, these cells will still be present in the supernatant and their viability will still be assessed. By contrast, the washing steps of the monolayer disruption assays would cause detached human cells to be removed, and thus, their viability would not be assessed.

The CellTiterGlo assay is robust and requires very few steps; thus, the procedure is amenable to high throughput screening. Indeed, CellTiterGlo has previously been used in a high throughput screen for drugs that kill *E. histolytica* [28]. Position effects, where some wells are less reliable, were not previously noted [28], and we also did not detect position effects in this assay. The chief limitation of this assay is that it does not directly measure human cell death. Because human cells greatly outnumber amoebae in this assay, they contribute the majority of the ATP to the readout, and thus, a decrease in luminescence can be inferred to represent human cell death. Also, similar to the limitations of apoptosis assays, ATP levels are correlated with dying cells, but do not clearly define the "point of no return" when a cell is by definition, dead [29, 30]. The depletion of ATP below a threshold, combined with redox alterations, has been proposed to mark the "point of no return" [31], however, it would be difficult to infer from an assay like CellTiterGlo that the level of ATP has definitively crossed a threshold. However, the major strengths of this assay are the simplicity and adaptability to high throughput approaches. This is an area where none of the existing cell death assays are useful. Thus, we propose that this assay is most useful for initial screening of mutants or candidate inhibitors. Finally, since monolayers can be grown directly in the plates used for this assay, it is easily adaptable to both monolayers and suspension cells.

The dual-stain microscopy-based cell death assay is also simple and practical. We used confocal microscopy for imaging, but this is not necessary, as widefield fluorescence microscopes can also be used. The major strength of this assay is that it directly measures human cell death. Dead cells are labeled, thus human cell death can be directly quantified within a mixture of human cells and amoebae. Moreover, the readout for cell death in this assay is loss of membrane integrity, which is a direct marker of cells that are dead [24]. Thus, this assay, together with the imaging flow cytometry assay that we developed [7], represent the most direct assays available for human cell killing for *E. histolytica.* The dual-stain assay is more practical and easier to apply, since imaging flow cytometers are not widely available.

Like imaging flow cytometry, the dual-stain assay can be applied to medium throughput approaches, as it could be performed by using cells in plates and by imaging on high content screening microscopes. We did not use plates when establishing this assay, but it could easily be adapted for use with 96- or 384-well plates. The limitation of this assay is that the readout is not inherently quantitative, and requires counting of labeled cell nuclei. We did not develop automated image analysis, but this would be possible, and would ensure that the readout is unbiased and efficient. Because both stains label the same cellular feature, the nucleus, automated image analysis should be particularly robust. Finally, like the CellTiterGlo assay, the dual-stain microscopy assay is amenable to both monolayer and suspension cell cultures.

Together, these assays expand the repertoire of available tools for studying trogocytosis by *E. histolytica.* They are particularly simple and practical, and thus we believe they are suitable for wide application. These assays also pave the way for high-throughput studies, and they could be adapted for use in 384-well plates. The two assays could potentially be combined such that cells are first visualized using the dual-stain assay, and are subsequently lysed and assayed with CellTiterGlo. Alternatively, the CellTiterGlo assay could be used as a primary screening tool, and the dual-stain assay could be used as a secondary screening tool. Very little is known about the specific molecular mechanism underlying trogocytosis, and thus, these assays pave the way for studies that will improve understanding of this process. Since trogocytosis by *E. histolytica* is likely to underlie disease pathogenesis, these tools are expected to allow for an improved understanding of the mechanism of disease, and may be applicable to the development of new therapeutics.

Supplementary Material

Refer to Web version on PubMed Central for supplementary material.

Acknowledgments

References

[1]. WHO/PAHO/UNESCO report. A consultation with experts on amoebiasis. Mexico City, Mexico 28–29 January, 1997 Epidemiol Bull, 1997. 18(1):13.

[2]. Gilchrist CA, Petri SE, Schneider BN, Reichman DJ, Jiang N, Begum S, Watanabe K, Jansen CS, Elliott KP, Burgess SL, Ma JZ, Alam M, Kabir M, Haque R, and Petri WA Jr. Role of the Gut Microbiota of Children in Diarrhea Due to the Protozoan Parasite Entamoeba histolytica. The Journal of infectious diseases, 2016 213(10):1579. [PubMed: 26712950]

[3]. GBD 2015 Mortality and Causes of Death Collaborators. Global, regional, and national life expectancy, all-cause mortality, and cause-specific mortality for 249 causes of death, 1980–2015: a systematic analysis for the Global Burden of Disease Study 2015. Lancet, 2016 388(10053):1459. [PubMed: 27733281]

[4]. Ravdin JI, Croft BY, and Guerrant RL. Cytopathogenic mechanisms of Entamoeba histolytica. J Exp Med, 1980 152(2):377. [PubMed: 6249882]

[5]. Ravdin JI and Guerrant RL. Role of adherence in cytopathogenic mechanisms of Entamoeba histolytica. Study with mammalian tissue culture cells and human erythrocytes. J Clin Invest, 1981 68(5):1305. [PubMed: 6271810]

[6]. Ralston KS and Petri WA Jr Tissue destruction and invasion by Entamoeba histolytica. Trends Parasitol, 2011 27(6):254. [PubMed: 21440507]

[7]. Ralston KS, Solga MD, Mackey-Lawrence NM, Somlata A Bhattacharya, and Petri WA Jr. Trogocytosis by Entamoeba histolytica contributes to cell killing and tissue invasion. Nature, 2014 508(7497):526. [PubMed: 24717428]

[8]. Ralston KS. Taking a bite: Amoebic trogocytosis in Entamoeba histolytica and beyond. Curr Opin Microbiol, 2015 28:26. [PubMed: 26277085]

[9]. Gilmartin A, Ralston K, and Petri WJ. Inhibition of Amebic Lysosomal Acidification Blocks Amebic Trogocytosis and Cell Killing. mBio, 2017 8(4)

[10]. Miller HW, Suleiman RL, and Ralston KS. Trogocytosis by Entamoeba histolytica Mediates Acquisition and Display of Human Cell Membrane Proteins and Evasion of Lysis by Human Serum. mBio, 2019 10(2)

[11]. Ravdin JI and Guerrant RL. Studies on the cytopathogenicity of Entamoeba histolytica. Arch. Invest. Med. (Mex), 1980 11:123. [PubMed: 6258505]

[12]. Li E, Stenson WF, Kunz-Jenkins C, Swanson PE, Duncan R, and Stanley SLJ. Entamoeba histolytica Interactions with Polarized Human Intestinal Caco-2 Epithelial Cells. Infection and Immunity, 1994 62(11):5112. [PubMed: 7927794]

[13]. Marie CS, Verkerke HP, Paul SN, Mackey AJ, Petri WA Jr. Leptin protects host cells from Entamoeba histolytica cytotoxicity by a STAT3-dependent mechanism. Infect Immun, 2012 80(5):1934. [PubMed: 22331430]

[14]. Riss T and Niles A, Moravec R, Karassina N, Vidugiriene J, Cytotoxicity Assays: In Vitro Methods to Measure Dead Cells Assay Guidance Manual, ed. G.A. Sittampalam GS, Brimacombe K, Arkin M, Auld D, Austin C, Baell J, Bejcek B, Caaveiro JMM, Chung TDY, Coussens NP, Dahlin JL, Devanaryan V, Foley TL, Glicksman M, Hall MD, Haas JV, Hoare SRJ, Inglese J, Iversen PW, Kahl SD, Kales SC, Kirshner S, Lal-Nag M, Li Z, McGee J, McManus O, Riss T, Trask OJ Jr., Weidner JR, Wildey MJ, Xia M, Xu X. 2019, Bethesda (MD): Eli Lilly & Company and the National Center for Advancing Translational Sciences.

[15]. Saffer LD and Petri WA. Role of the galactose lectin of Entamoeba histolytica in adherence-dependent killing of mammalian cells. Infection and Immunity, 1991 59(12):4681. [PubMed: 1937828]

[16]. Huston CD, Houpt ER, Mann BJ, Hahn CS, and Petri WA Jr. Caspase 3-dependent killing of host cells by the parasite Entamoeba histolytica. Cellular Microbiology, 2001 2(6)

[17]. Tillack M, Nowak N, Lotter H, Bracha R, Mirelman D, Tannich E, and Bruchhaus I. Increased expression of the major cysteine proteinases by stable episomal transfection underlines the important role of EhCP5 for the pathogenicity of Entamoeba histolytica. Molecular and Biochemical Parasitology, 2006 149(1):58. [PubMed: 16753229]

[18]. Bracha R and Mirelman D. Virulence of Entamoeba histolytica trophozoites. J. Exp. Med, 1984 160:353. [PubMed: 6088660]

[19]. Teixeira JE, Sateriale A, Bessoff KE, and Huston CD. Control of Entamoeba histolytica Adherence Involves Metallosurface Protease 1, an M8 Family Surface Metalloprotease with Homology to Leishmanolysin. Infect Immun, 2012 80(6):2165. [PubMed: 22451519]

[20]. Welter BH, Powell RR, Leo M, Smith CM, and Temesvari LA. A unique Rab GTPase, EhRabA, is involved in motility and polarization of Entamoeba histolytica cells. Mol Biochem Parasitol, 2005 140(2):161. [PubMed: 15760656]

[21]. Ravdin JI, Murphy CF, Guerrant RL, and Long-Krug SA. Effect of Antagonists of Calcium and Phospholipase A on the Cytopathogenicity of Entamoeba histolytica. The Journal of Infectious Diseases, 1985 152(3):542. [PubMed: 2863317]

[22]. Bracha R, Nuchamowitz Y, Leippe M, and Mirelman D. Antisense inhibition of amoebapore expression in Entamoeba histolytica causes a decrease in amoebic virulence. Molecular Microbiology, 1999 34(3):463. [PubMed: 10564488]

[23]. Seydel K and Stanley SJ. Entamoeba histolytica induces host cell death in amebic liver abscess by a non-Fas-dependent, non-tumor necrosis factor alpha-dependent pathway of apoptosis. Infect Immun, 1998 66(6):2980. [PubMed: 9596776]

[24]. Kroemer G, Galluzzi L, Vandenabeele P, Abrams J, Alnemri ES, Baehrecke EH, Blagosklonny MV, El-Deiry WS, Golstein P, Green DR, Hengartner M, Knight RA, Kumar S, Lipton SA, Malorni W, Nuñez G, Peter ME, Tschopp J, Yuan J, Piacentini M, Zhivotovsky B, and Melino G. Classification of cell death: recommendations of the Nomenclature Committee on Cell Death 2009. Cell Death & Differentiation, 2008 16(1):3. [PubMed: 18846107]

[25]. Petri WA Jr., Haque R, and Mann BJ. The bittersweet interface of parasite and host: lectin-carbohydrate interactions during human invasion by the parasite Entamoeba histolytica. Annu Rev Microbiol, 2002 56:39. [PubMed: 12142490]

[26]. Baxt LA, Baker RP, Singh U, and Urban S. An Entamoeba histolytica rhomboid protease with atypical specificity cleaves a surface lectin involved in phagocytosis and immune evasion. Genes Dev, 2008 22(12):1636. [PubMed: 18559479]

[27]. Baxt LA, Rastew E, Bracha R, Mirelman D, and Singh U. Downregulation of an Entamoeba histolytica rhomboid protease reveals roles in regulating parasite adhesion and phagocytosis. Eukaryot Cell, 2010 9(8):1283. [PubMed: 20581296]

[28]. Debnath A, Parsonage D, Andrade RM, He C, Cobo ER, Hirata K, Chen S, García-Rivera G, Orozco E, Martínez MB, Gunatilleke SS, Barrios AM, Arkin MR, Poole LB, McKerrow JH, and Reed SL. A high-throughput drug screen for Entamoeba histolytica identifies a new lead and target. Nature Med, 2012 18(6):956. [PubMed: 22610278]

[29]. Leist M, Single B, Castoldi AF, Kuhnle S, and Nicotera P. Intracellular Adenosine Triphosphate (ATP) Concentration: A Switch in the Decision Between Apoptosis and Necrosis. Journal of Experimental Medicine, 1997 185(8)

[30]. Bonora M, Patergnani S, Rimessi A, De Marchi E, Suski JM, Bononi A, Giorgi C, Marchi S, Missiroli S, Poletti F, Wieckowski MR, and Pinton P. ATP synthesis and storage. Purinergic Signal, 2012 8(3):343. [PubMed: 22528680]

[31]. Galluzzi L, Bravo-San Pedro JM, Vitale I, Aaronson SA, Abrams JM, Adam D, Alnemri ES, Altucci L, Andrews D, Annicchiarico-Petruzzelli M, Baehrecke EH, Bazan NG, Bertrand MJ, Bianchi K, Blagosklonny MV, Blomgren K, Borner C, Bredesen DE, Brenner C, Campanella M, Candi E, Cecconi F, Chan FK, Chandel NS, Cheng EH, Chipuk JE, Cidlowski JA, Ciechanover A, Dawson TM, Dawson VL, De Laurenzi V, De Maria R, KM Debatin, Di Daniele N, Dixit VM, Dynlacht BD, El-Deiry WS, Fimia GM, Flavell RA, Fulda S, Garrido C, Gougeon ML, Green DR, Gronemeyer H, Hajnoczky G, Hardwick JM, Hengartner MO, Ichijo H, Joseph B, Jost PJ, Kaufmann T, Kepp O, Klionsky DJ, Knight RA, Kumar S, Lemasters JJ, Levine B, Linkermann A, Lipton SA, Lockshin RA, Lopez-Otin C, Lugli E, Madeo F, Malorni W, Marine JC, Martin SJ, Martinou JC, Medema JP, Meier P, Melino S, Mizushima N, Moll U, Munoz-Pinedo C, Nunez G, Oberst A, Panaretakis T, Penninger JM, Peter ME, Piacentini M, Pinton P, Prehn JH, Puthalakath H, Rabinovich GA, Ravichandran KS, Rizzuto R, Rodrigues CM, Rubinsztein DC, Rudel T, Shi Y, Simon HU, Stockwell BR, Szabadkai G, Tait SW, Tang HL, Tavernarakis N, Tsujimoto Y, Vanden Berghe T, Vandenabeele P, Villunger A, Wagner EF,

Walczak H, White E, Wood WG, Yuan J, Zakeri Z, Zhivotovsky B, Melino G and Kroemer G. Essential versus accessory aspects of cell death: recommendations of the NCCD 2015. Cell Death Differ, 2015 22(1):58. [PubMed: 25236395]

[32]. Morf L RJ Pearson AS Wang, and Singh U. Robust gene silencing mediated by antisense small RNAs in the pathogenic protist Entamoeba histolytica. Nucleic Acids Research, 2013 41(20):9424. [PubMed: 23935116]
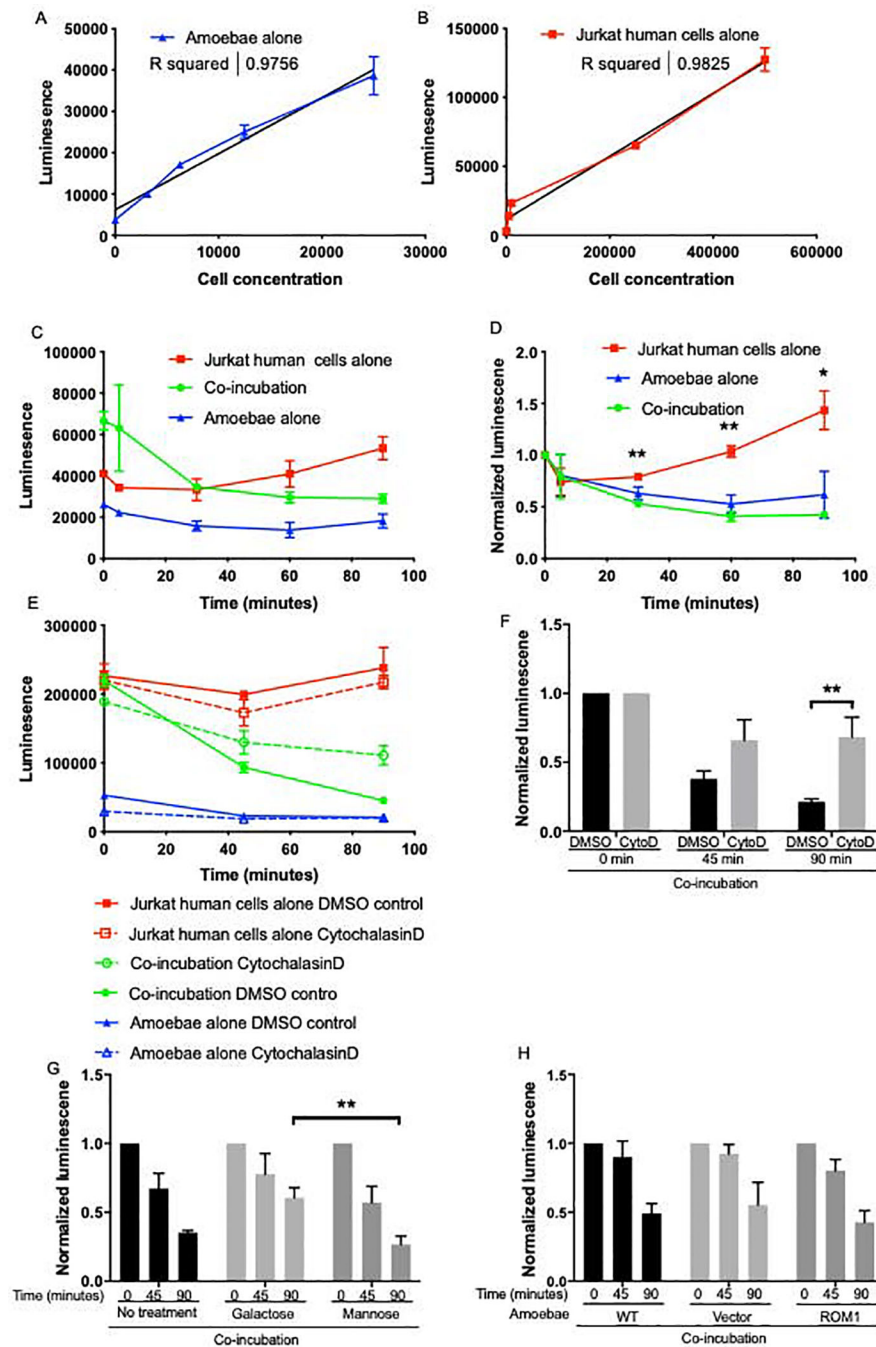
Highlights

- Two ways to measure killing of human cells by *Entamoeba histolytica* were developed.

- One assay measures ATP levels, and is amenable to high-throughput approaches.

- The second assay uses two fluorescent stains to directly detect dead human cells.

- These assays are tools to understand trogocytosis and amoebiasis pathogenesis.

Figure 1: CellTiterGlo can be used to assay Jurkat cell killing by amoebae.

E. histolytica HM1:IMSS trophozoites and Jurkat T cells were each cultured and harvested as described [7, 10]. Cells were first washed in fresh TYI media [7, 10], and then incubated in 96 well plates (Corning 3603) in an anaerobic GasPak (BD) at 35°C. The CellTiterGlo assay (Promega) was carried out according to the manufacturer's instructions. Two wells for each condition were averaged to generate one value per condition, and at least three experiments were performed independently on different days. **(A)** A dilution series of amoebae, or **(B)** human Jurkat T cells was assayed using CellTiterGlo. Best fit lines and R^2

values are shown. CellTiterGlo signal correlates with the number of cells per well. Data represent the average values of two replicate wells for each cell concentration, and are representative of 3 independent experiments. **(C)** Amoebae were co-incubated (filled circles) with Jurkat cells at a 1:5 ratio, or amoebae (filled triangles) and Jurkat cells (filled squares) were incubated separately as controls. Data represent the average values of two replicate wells for each sample, from one experiment. **(D)** Data from 2 independent experiments performed as in Panel C were normalized to the value of each sample at Time = 0. There were statistically significant differences between the co-incubation and Jurkat alone samples, as indicated. **(E)** Amoebae and human Jurkat T cells were treated with Cytochalasin D (open symbols) or DMSO (filled symbols). Cells were first washed in fresh TYI media and pretreated with 20 nM Cytochalasin D (Sigma Aldrich) or an equivalent volume of DMSO for 1 hour at 35°C. Cytochalasin D, or DMSO, was maintained at the same concentration during the CellTiterGlo assay. Amoebae were co-incubated (circles) with Jurkat cells at a 1:20 ratio, or amoebae (triangles) and Jurkat cells (squares) were incubated separately as controls. Viability was assayed by using CellTiterGlo. Data represent the average values of two replicate wells for each sample, from one experiment. **(F)** Data from 4 independent experiments performed as in panel A were normalized to the value of each sample at Time = 0. **(G)** Amoebae and Jurkat cells were incubated in media containing galactose, mannose, or no added sugar. Cells were first resuspended in fresh TYI media with no supplementation, 100 mM galactose (Sigma Aldrich), or 100 mM mannose (Sigma Aldrich); sugars were maintained at the same concentration during the CellTiterGlo assay. Cells were co-incubated at a 1:20 ratio, or incubated separately as controls. Viability was assayed by using CellTiterGlo. Data from 3 independent experiments were normalized to the value of each sample at Time = 0. **(H)** Amoebae were transfected with an EhRom1 knockdown plasmid, or a vector control plasmid. The EhROM1 silencing construct was generated by Morf, *et al.* [32], and contains 132 base pairs of the trigger gene (EHI_048600) fused to the first 537 base pairs of EhROM1 (EHI_197460). Stable transfectants were obtained, cloned by limiting dilution, and assessed for knockdown using RT-PCR as described [10]. Transfectants, or wild-type non-transfected amoebae, were co-incubated with Jurkat cells at a 1:20 ratio, or incubated separately as controls. Data from 3 independent experiments were normalized to the value of each sample at Time = 0. GraphPad Prism was used to calculate best fit line and R^2 values, and for student's unpaired *t* test statistical analysis. Mean values and standard deviations are shown; ns = P > 0.05, * = P < 0.05, ** = P < 0.01, *** = P < 0.001, **** = P < 0.0001.
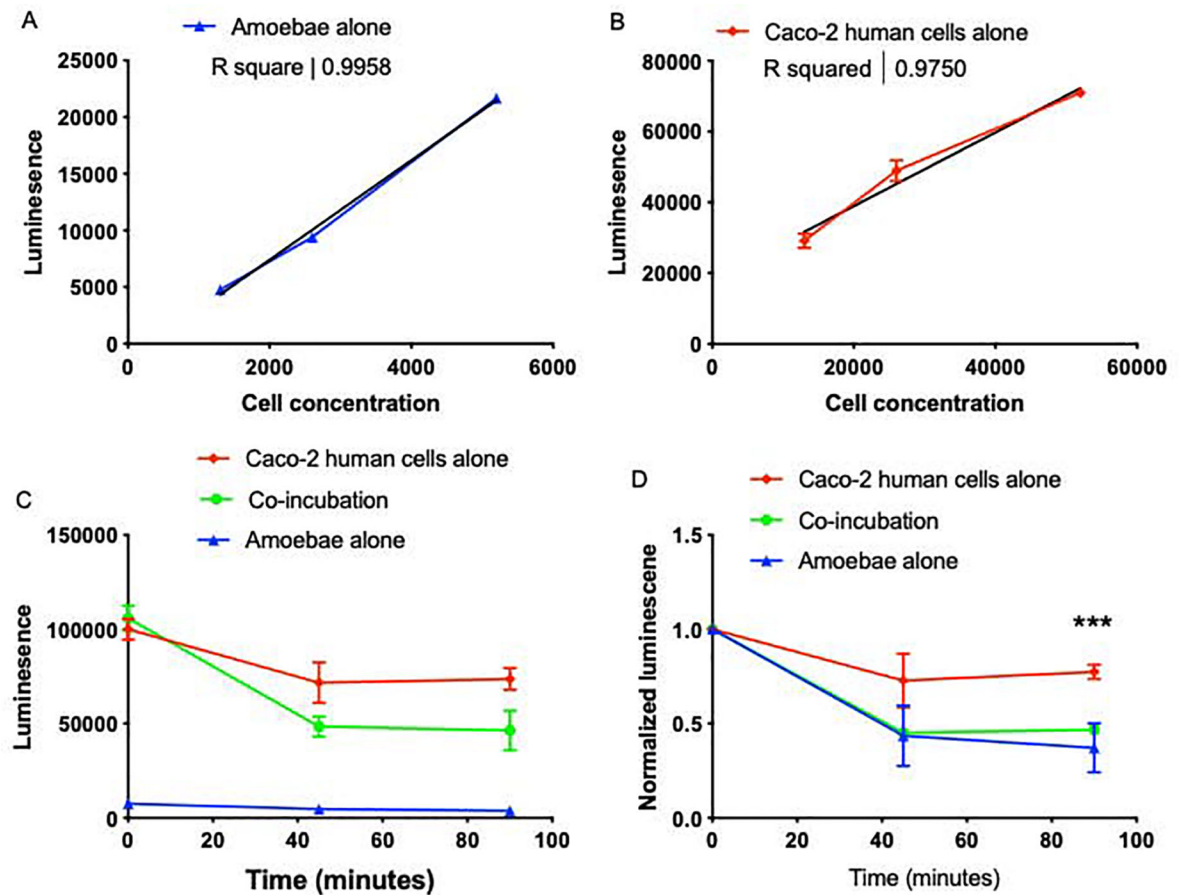
Figure 2: CellTiterGlo can be used to assay Caco-2 cell killing by amoebae.
Caco-2 cells were cultured and harvested as described [7]. 18–24 hours prior to performing
the experiment, Caco-2 cells were plated in 96-well plates. On the day of the experiment,
cells were washed with fresh TYI. Amoebae were added to create approximate co-
incubation ratio of 1 amoeba: 10 Caco-2 cells. The CellTiterGlo assay (Promega) was
carried out according to the manufacturer's instructions. Three wells of amoebae alone, six
wells of Caco-2 cells alone, and six wells of co-incubated samples were averaged to obtain
one value per condition, and three experiments were performed independently on different
days. **(A)** A dilution series of amoebae, or **(B)** human Caco-2 intestinal epithelial cells were
assayed using CellTiterGlo. Best fit lines and R^2 values are shown. CellTiterGlo signal
correlates with the number of cells per well. Data represent the average values of two
replicate wells for each cell concentration, and are representative of 3 independent
experiments. **(C)** Amoebae were co-incubated (filled circles) with Caco-2 cells at an
approximately 1:10 ratio, or amoebae (filled triangles) and Caco-2 cells (filled squares) were
incubated separately as controls. Data represent the average values of two replicate wells for
each sample, from one experiment. **(D)** Data from 3 independent experiments performed as
in panel C were normalized to the value of each sample at Time = 0. There were statistically
significant differences between the co-incubation and Caco-2 alone samples, as indicated.
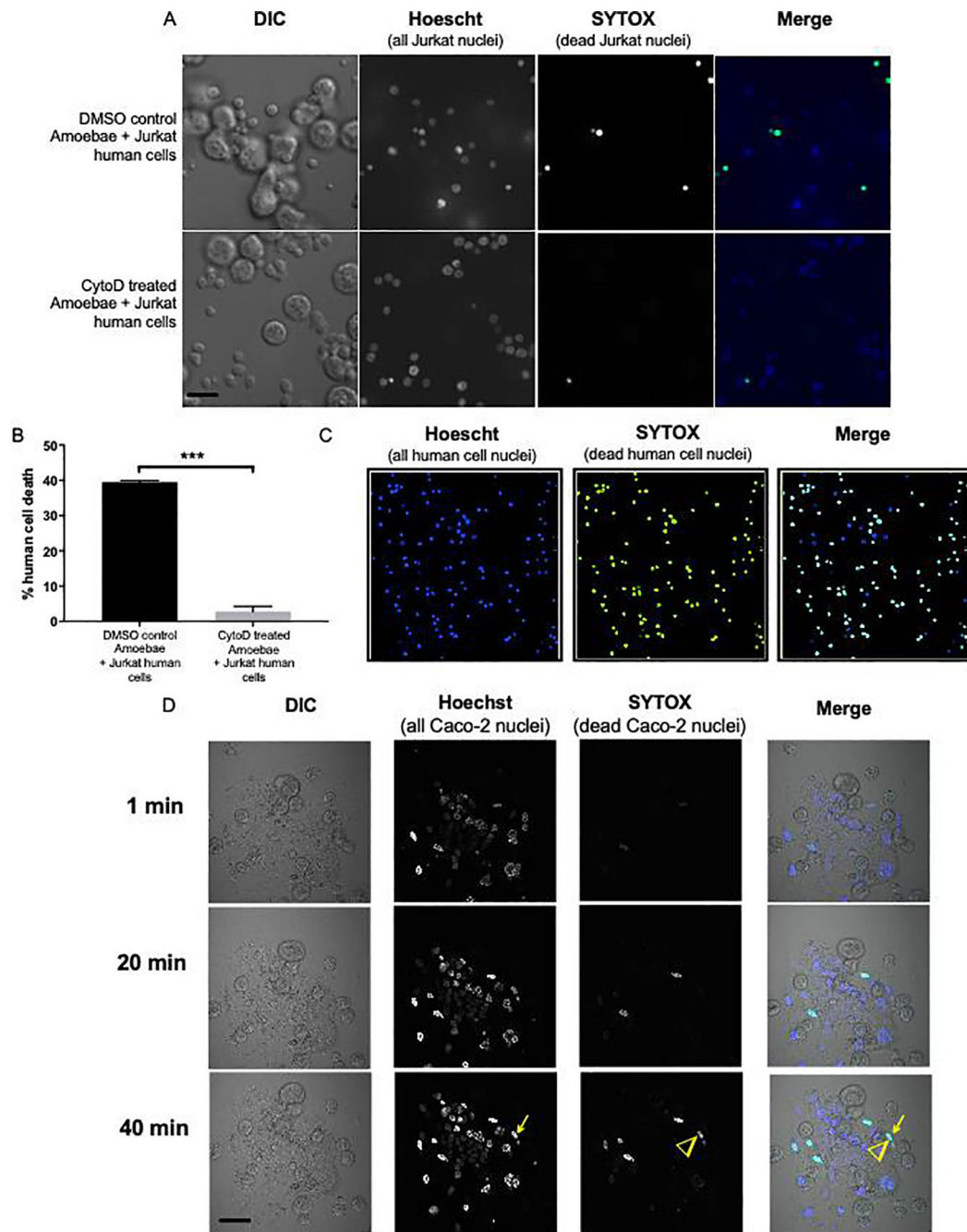GraphPad Prism was for student's unpaired *t* test statistical analysis. Mean values and

standard deviations are shown; ns = P > 0.05, * = P < 0.05, ** = P < 0.01, *** = P < 0.001, **** = P < 0.0001.

Figure 3: A dual-stain microscopy assay can be used to quantitatively and directly detect human cell killing by amoebae.

Human cells were pre-labeled with Hoechst 33342 (Invitrogen) at 5 μg/ml for 30 minutes at 37°C. Amoebae and human cells were then co-incubated in glass bottom petri dishes (MatTek) for 60 minutes at 35°C in M199s media [7, 10] containing 20 nM SYTOX green (Invitrogen). For experiments using Caco-2 cells, Caco-2 cells were cultured on collagen-coated glass bottom petri dishes and experiments were performed when cells were ~80% confluent. Cells were imaged using a stage warmer set to 35°C on either an Intelligent Imaging Innovations hybrid spinning disk confocal microscope or an Olympus FV1000 laser

point-scanning confocal microscope. Two experiments were performed independently on different days, and 350–500 human cells were counted for each condition. **(A)** Amoebae and Hoechst-labeled human Jurkat T cells were pre-treated with 20 nM Cytochalasin D or an equivalent volume of DMSO for 1 hour at 35°C. Representative images are shown. Living human cells are labeled by Hoechst (blue), while dead human cells are labeled by both Hoechst and SYTOX green (green) and appear as turquoise in the merged image. An example of a living cell (arrow) and a dead cell (arrowhead) are indicated. Scale bar, 50 μm. **(B)** Human cell death was assayed by quantifying the number of single-stained (Hoechst) and dual-stained (Hoechst and SYTOX green) human cell nuclei, which correspond to living and dead human cells, respectively. Data are representative of 2 independent experiments. **(C)** Representative images demonstrating that the dual-stain assay can be applied to low magnification objectives, allowing for a greater number of cells to be imaged per field. Scale bar, 50 μm. **(D)** Amoebae and Hoechst-labeled human Caco-2 intestinal epithelial cells were co-incubated in the presence of SYTOX green. Cells were imaged live, over a time course. The full time course is shown in Fig. S3 and Videos S2 – S3. The arrow indicates an example of a Caco-2 cell that is initially living and labeled only by Hoechst, but is eventually killed by an amoeba, at which time it becomes labeled by SYTOX green (arrowhead). Data are representative of 2 independent experiments. Scale bar, 50 μm. GraphPad Prism was used for student's unpaired t test statistical analysis. Mean values and standard deviations are shown; ns = $P > 0.05$, * = $P < 0.05$, ** = $P < 0.01$, *** = $P < 0.001$, **** = $P < 0.0001$.

Author Manuscript

Author Manuscript

Author Manuscript

Author Manuscript